2-2003

Five-Member Gene Family of Bartonella Quintana

Michael F. Minnick
University of Montana - Missoula, mike.minnick@mso.umt.edu

Kate N. Sappington

Laura S. Smitherman

Siv G. E. Andersson

Olof Karlberg

See next page for additional authors

INFECTION AND IMMUNITY, Feb. 2003, p. 814–821 Vol. 71, No. 2
0019-9567/03/$08.00+0 DOI: 10.1128/IAI.71.2.814–821.2003

Five-Member Gene Family of *Bartonella quintana*

Michael F. Minnick,[1]* Kate N. Sappington,[1] Laura S. Smitherman,[1] Siv G. E. Andersson,[2] Olof Karlberg,[2] and James A. Carroll[3]

Division of Biological Sciences, The University of Montana, Missoula, Montana 59812[1]; Department of Molecular Evolution, Evolutionary Biology Center, Uppsala University, Uppsala, Sweden[2]; and Microscopy Branch, Rocky Mountain Laboratories, National Institute of Allergy and Infectious Diseases, Hamilton, Montana 59840[3]

Received 16 September 2002/Returned for modification 10 October 2002/Accepted 1 November 2002

***Bartonella quintana*, the agent of trench fever and an etiologic agent of bacillary angiomatosis, has an extraordinarily high hemin requirement for growth compared to other bacterial pathogens. We previously identified the major hemin receptor of the pathogen as a 30-kDa surface protein, termed HbpA. This report describes four additional homologues that share approximately 48% amino acid sequence identity with *hbpA*. Three of the genes form a paralagous cluster, termed *hbpCAB*, whereas the other members, *hbpD* and *hbpE*, are unlinked. Secondary structure predictions and other evidence suggest that Hbp family members are β-barrels located in the outer membrane and contain eight transmembrane domains plus four extracellular loops. Homologs from a variety of gram-negative pathogens were identified, including *Bartonella henselae* Pap31, *Brucella* Omp31, *Agrobacterium tumefaciens* Omp25, and neisserial opacity proteins (Opa). Family members expressed in vitro-synthesized proteins ranging from ca. 26.5 to 35.1 kDa, with the exception of HbpB, an ~55.9-kDa protein whose respective gene has been disrupted by a ~510 GC-rich element containing variable-number tandem repeats. Transcription analysis by quantitative reverse transcriptase-PCR (RT-PCR) indicates that all family members are expressed under normal culture conditions, with *hbpD* and *hbpB* transcripts being the most abundant and the rarest, respectively. Mutagenesis of *hbpA* by allelic exchange produced a strain that exhibited an enhanced hemin-binding phenotype relative to the parental strain, and analysis by quantitative RT-PCR showed elevated transcript levels for the other *hbp* family members, suggesting that compensatory expression occurs.**

Bartonella quintana is the bacterial agent of trench fever and is transmitted between humans by the bite of the human body louse (*Pediculus humanis*) (5). *B. quintana* was a major cause of morbidity during World Wars I and II and is reemerging as a secondary infectious agent primarily in immunocompromised patients and a cause of "urban trench fever" in homeless, inner-city dwellers (11, 12). *B. quintana* infections can manifest as typical trench fever (11), bacillary angiomatosis (13), chronic bacteremia (24), endocarditis (23), lymphadenpathy (13), or infections of the nervous and skeletal systems (13, 18). These conditions can occur concurrently and may be life-threatening.

Very little is known of *B. quintana*'s virulence determinants, epidemiology, or the reason for its reemergence. It is known that this bacterium has a high requirement for hemin. Investigation into this extraordinary hemin requirement led to our identification and characterization of a major hemin-binding protein, hemin-binding protein A (HbpA), from *B. quintana* (6). HbpA is a heat-modifiable outer surface protein that retains its ability to bind hemin after sodium dodecyl sulfate-polyacrylamide gel electrophoresis (SDS-PAGE).

We have determined that *hbpA* belongs to a gene family consisting of five genes. Here we describe the four additional members of this multigenic family, and report the first successful site-directed mutagenesis and *trans*-complementation in this *Bartonella* species using *hbpA* as the gene target. We use quantitative reverse transcription-PCR (RT-PCR) to determine the relative transcript level of each *hbp* gene family member and compare transcript levels in the wild-type to that of the *hbpA* mutant.

* Corresponding author. Mailing address: Division of Biological Sciences, The University of Montana, Missoula, MT 59812-4824. Phone: (406) 243-5972. Fax: (406) 243-4184. E-mail: minnick@selway.umt.edu.

MATERIALS AND METHODS

Bacterial strains and culture conditions. *B. quintana* was grown on heart infusion agar blood plates (HIAB [6]) at 37°C in 5% CO_2 and 100% relative humidity and was harvested at 3 days postinoculation (approximately mid-log phase [32]). *E. coli* was grown in Luria-Bertani medium for 16 h at 37°C. When required, antibiotic supplements were added to the medium at standard concentrations (21). *B. quintana* and *Escherichia coli* strains used or generated in this study are summarized in Table 1.

Preparation and manipulation of nucleic acids. Plasmids used or generated in this study are listed in Table 1. Plasmids intended for routine use were purified from *E. coli* with a Perfectprep kit (Eppendorf Scientific, Westbury, N.Y.). Plasmids used in sequencing, in vitro transcription-translation, or electroporation were prepared with a Midi-Prep kit (Qiagen, Valencia, Calif.). Genomic DNA was prepared by a hexadecyltrimethyl ammonium bromide technique (2). RNA was isolated using an Ultraspec-II RNA isolation system (Biotex, Huston, Tex.) and contaminating DNA was removed using DNA-Free from Ambion (Austin, Tex.). RNA purity was assayed by a standard protocol (2). Clonings, ligations, and transformation reactions with *E. coli* were performed as previously described (6).

Nucleotide sequencing and analysis. Both DNA strands were sequenced using a BigDye Terminator Cycle Sequencing Ready Reaction Kit (Applied Biosystems, Inc. [ABI]/Roche, Branchburg, N.J.) and an automated DNA sequencer (ABI; model 377). Sequence data were compiled and analyzed with Seqweb version 2.0 (Accelrys, San Diego, Calif.) or the National Center for Biotechnology Information website (http://www.ncbi.nlm.nih.gov/). BLAST 2.0 (1) was used for database searches, whereas sequence alignments were done with FASTA 2.0

TABLE 1. Bacterial strains and plasmids used in this study

Strain or plasmid	Relevant characteristic(s)	Source or reference
Strains		
B. quintana		
OK 90-268	Human isolate	CDC[a]
LS100	OK 90-268 transformed with pEST	This study
LS200	LS100 cured of pEST	This study
LS300	*hbpA* in LS200 disrupted by pHBPA′	This study
LS400	LS300 *trans*-complemented for *hbpA* using pBBR1-HBPA	This study
E. coli DH5α	Host strain for cloning	Gibco-BRL
Plasmids		
pEST	Replicon for *B. quintana*	20
pBluescript SK (+/−)	Cloning vector	Stratagene
pBK-CMV	Excised vector from λ Zap	Stratagene
pUB1	*Bartonella* suicide vector	3
pBBR1-MCS	*Bartonella* shuttle vector	3
pHBPA′	Suicide vector-pUB1 containing *hbpA′*	This study
pBBR1-HBPA	pBBR1-MCS containing *hbpA*	This study
pHBP-CMV	pBK-CMV containing *hbpA*	6
pHBPB	pBluescript SK containing *hbpB*	This study
pHBPC	pBluescript SK containing *hbpC*	This study
pHBPD	pBluescript SK containing *hbpD*	This study
pHBPE	pBluescript SK containing *hbpE*	This study

[a] CDC, Centers for Disease Control and Prevention, Atlanta, Ga.

(19), CLUSTALW 1.6 (26), and BOXSHADE 3.21 (K. Hoffman and M. D. Baron [www.ch.embnet.org/software/BOX_form.html], 1998).

SDS-PAGE, immunoblots, and N-terminal sequencing. Protein samples (20 μg total) were separated on SDS-PAGE gels (12.5% [wt/vol] acrylamide) prepared by standard protocol (2). For immunoblots, gels were transferred overnight to supported nitrocellulose (0.45-μm pore size; Osmonics, Minnetonka, Minn.) by the general methods of Towbin et al. (27). The resulting blot was probed by using rabbit anti-HbpA antiserum prepared as before (6) and subsequently developed by using horseradish peroxidase-conjugated goat anti-rabbit immunoglobulin G antibody (Sigma), H_2O_2, and 4-chloronapthol as previously detailed (22). For N-terminal sequencing, a Triton X-114 precipitate was prepared from *B. quintana* as previously described (6) and transferred to polyvinylidene difluoride (16). The polyvinylidene difluoride was stained for 15 min with 0.05% Coomassie blue and rinsed briefly, and then the HbpD protein band excised, dried, and subjected to Edman degradation by using an ABI 431A automated peptide sequencer. Sequencing was performed on two separate samples.

Mutagenesis and *trans*-complementation of *hbpA*. Mutagenesis of *B. quintana* was done by using a strategy we previously described for *Bartonella bacilliformis* (3). Briefly, a transformation-competent strain of *B. quintana* (L200) was prepared by electroporating wild-type *B. quintana* (OK 90-268) with pEST. Transformants were subsequently selected on HIAB-Kan plates (i.e., HIAB plus 25 μg of kanamycin/ml) and one resulting strain (LS100) was cured of pEST by six serial culture passages on HIAB. The resulting strain, LS200, was verified as cured of pEST by PCR analysis and kanamycin sensitivity as previously described (3). LS200 was subsequently electroporated with a suicide vector containing a 240-bp internal fragment of *hbpA* (nucleotides 344 to 583), termed pHBPA′. Mutants were selected on HIAB-Kan. One resulting strain, LS300, was verified as a *hbpA* mutant by PCR, SDS-PAGE, and immunoblotting. Finally, LS300 was complemented in *trans* by transforming with the shuttle vector, pBBR1-HBPA, to generate strain LS400.

Hemin-binding assay. Hemin binding by intact *B. quintana* cells was assayed in vitro essentially as before (6). Briefly, eight plates of *B. quintana* were harvested into 1.0 ml of 100 mM Tris (pH 8.0) and washed four times by centrifuging the suspension for 5 min at 2,940 × *g* and resuspending the resulting pellet into 1.0 ml of 100 mM Tris (pH 8.0). The final pellet was resuspended to an optical density at 600 nm (OD_{600}) of 1.0, and four 1-ml aliquots were obtained from each strain. A total of 5 μg of hemin (5 μl of a fresh 1-mg/ml hemin stock solution in 0.02 N NaOH) were added to each tube, gently mixed, and incubated open for 1 h at 37°C at 5% CO_2, with gentle mixing at 15-min intervals. Four negative control tubes without *B. quintana* cells were prepared and incubated as well. After incubation, the suspensions were pelleted by centrifuging for 2 min at 16,000 × *g*, and the resulting supernatants clarified twice by transferring to new microcentrifuges tube and centrifuging again at 16,000 × *g*. The OD_{400} of the final supernatants was assayed, and hemin binding was determined by comparing the reduction in OD_{400} to negative controls.

In vitro transcription-translation. Plasmids containing individual *hbp* genes plus their respective promoters were directionally cloned into pBluescript SK(+/−) in opposite orientation to the *lacZ* promoter. The resulting plasmids (Table 1) were used as templates for a S30 extract kit for circular DNA per the manufacturer's instructions (Promega, Madison, Wis.). Proteins were radiolabeled with a [^{35}S]cysteine-methionine mix (Express; New England Nuclear, Boston, Mass.). Translation products were separated on SDS-PAGE (12.5% [wt/vol] acrylamide) and visualized by exposure of the dried gel to X-ray film overnight.

RT-PCR quantification of *hbp* family transcripts. Quantitative RT-PCR was performed using TaqMan One-Step RT-PCR master mix from ABI. Ten-microliter reactions were performed in triplicate in a 384-well format, and reactions contained 500 nM concentrations of each primer, 100 nM probe, Master Mix and MultiScribe, and RNase inhibitor Mix to 1× (ABI); RNA was then serially diluted twofold from 5 ng per reaction to 0.153 ng per reaction. Probes consisted of an oligonucleotide labeled at the 5′ end with the reporter dye 5-carboxyfluorescein and at the 3′ end with the quencher *N,N′,N′*-tetramethyl-6-carboxyrhodamine. Primers and probes used in this study are listed in Table 2. Quantitative RT-PCR conditions were as follows: 1 cycle at 50°C for 30 min, 1 cycle at 95°C for 10 min, and 40 cycles of 95°C for 15 s and of 60°C for 60 s. Changes in fluorescence were monitored by using an ABI 7900HT sequence detection system and raw data were analyzed by SDS software version 2.0 (ABI). Chromosomal DNA from *B. quintana* was used as a control to ensure that the primers or probe from each gene were binding at similar efficiencies. The efficiency of primers or probe binding was determined by linear regression by plotting the cycle threshold (C_T) value versus the log of the RNA dilution. The slopes for all reactions were determined to be similar, indicating similar reaction efficiencies. Relative quantification of transcript was determined using the comparative C_T method ($2^{-\Delta\Delta C_T}$) calibrated to 16S rRNA (14). Quantitative RT-PCR experiments were performed multiple times independently with comparable results.

TABLE 2. Primers and probes designed for TaqMan analysis of the *hbp* gene family

Target gene	Sequence (5′-3′)		
	Forward primer	Reverse primer	Fluorescent probe[a]
16 S rRNA	TGTTAGCCGTCGGGTGGTT	CCCCAGGCGGAATGTTTAA	ACTACTCGGTGGCGCAGCTAACGC
hbpA	TGATGGTTGGTTTTACCGTTAGTG	ATTCTCCACGCAGCAAAACAT	TCCGGTCATTGCAACATCAACACCA
hbpB	CATCAGTCAGCACCAACTTCTTTG	ATTTGAATCCCTGCATAAAAACCT	CAGTTATTGCAGCTCCTGCTTTTACC
hbpC	GGATGACCTTTTGCCTAAATTGTC	GACCATTGCCGAGATCAACA	AGAGCCGACATAAATGCCACCCATC
hbpD	GGGAGCGCTTGATGCCTTA	CGGTGCTACAAAAGTATTTTGAATCT	ATTGCTGGAGGTGTTGCTTATACG
hbpE	CACACGAGTGCGAGTTGGTT	TGAAACTGCCCATAAGCAACAC	TTGAGCGTATGATGCCGTATATCTC

[a] Covalently linked at the 5′ end to 5-carboxyfluorescein and at the 3′ end to *N,N′,N′*-tetramethyl-6-carboxyrhodamine.

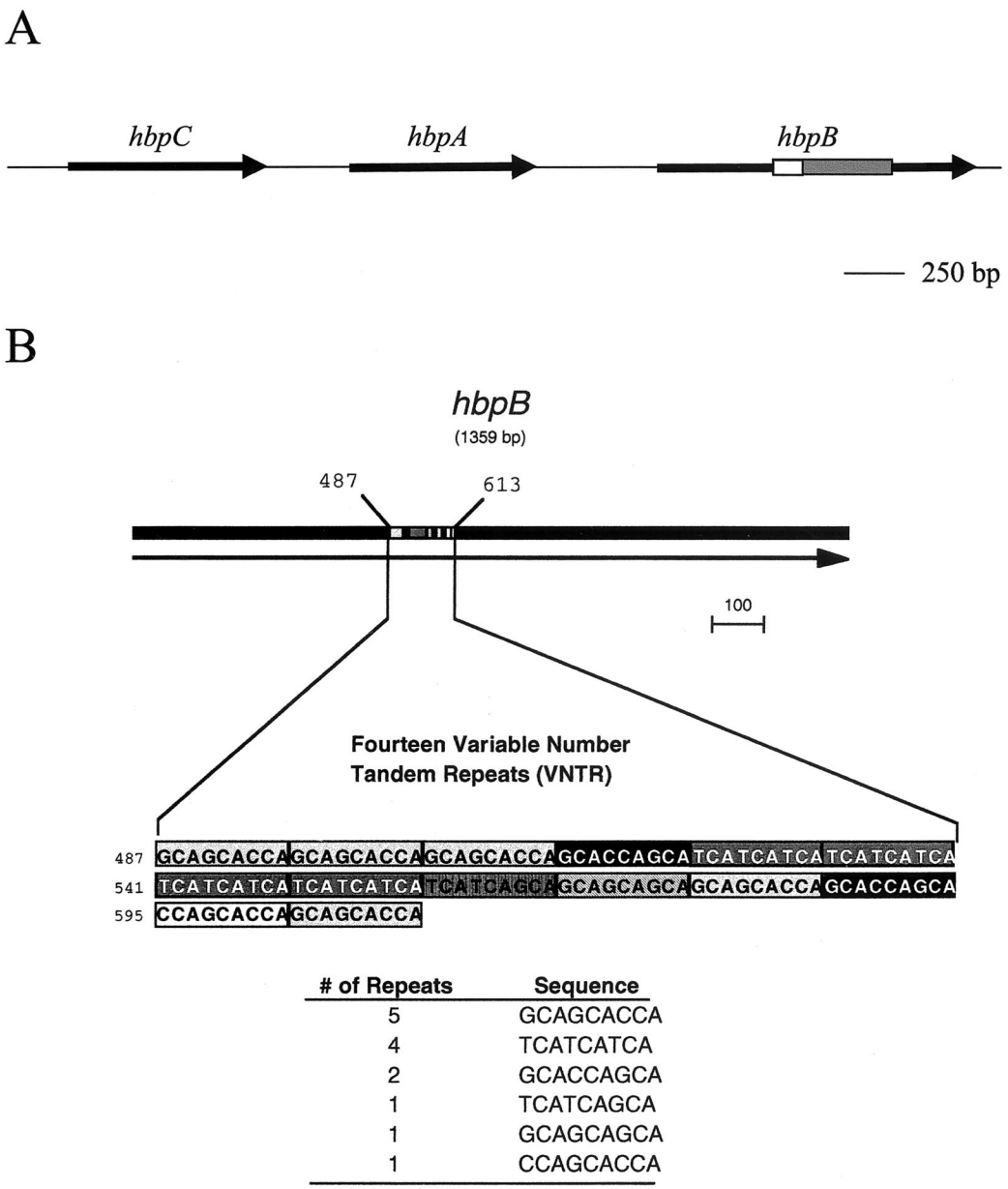

# of Repeats	Sequence
5	GCAGCACCA
4	TCATCATCA
2	GCACCAGCA
1	TCATCAGCA
1	GCAGCAGCA
1	CCAGCACCA

FIG. 1. (A) Linkage map of the *hbpCAB* locus of *B. quintana*. Arrows indicate the positions of the open reading frames in the gene cluster. The gray box in *hbpB* indicates the position of the 510-bp insert with its nested 126-bp tandem repeat region shown as a white box (see Fig. 1B). (B) Variable-number tandem repeat region of *hbpB*. The number of repeats and their respective sequences are indicated.

Statistical analysis. Student's *t* test results, standard error of the mean values, and graphs were generated with SigmaPlot 3.0 software (Jandel Scientific, San Rafael, Calif.). A P value of <0.05 was considered significant.

Nucleotide sequence accession numbers. GenBank accession numbers for the sequence data reported in this paper include: *hbpA* (AF266281), the *hbpCAB* locus (AY126673), *hbpD* (AY126674), and *hbpE* (AY126675).

RESULTS

Discovery of the *hbp* gene family. Sequence analysis of DNA flanking the *hbpA* gene revealed two closely linked homologs in the same orientation, designated *hbpB* and *hbpC*. This paralogous cluster of genes forms the *hbpCAB* locus (Fig. 1A). In addition to *hbpCAB*, two unlinked homologs, termed *hbpD* and *hbpE*, were subsequently identified using sequence data from the *B. quintana* genome project (O. Karlberg, B. Legault, K. Naslund, A. S. Eriksson, B. Lascola, M. Holmberg, and S. G. E. Andersson, unpublished data), bringing the *hbp* family membership to five genes.

The *hbpC*, *hbpD*, and *hbpE* genes are 831, 882, and 897 bp in length, respectively; values that are similar to the 816-bp *hbpA* gene (6). In contrast, the *hbpB* gene is 1,359 bp in length due to a ~510-bp insert near the center of its open reading frame (Fig. 1A). This insert contains a nested 126-bp variable-number tandem repeat region comprised of 14 in-frame re-

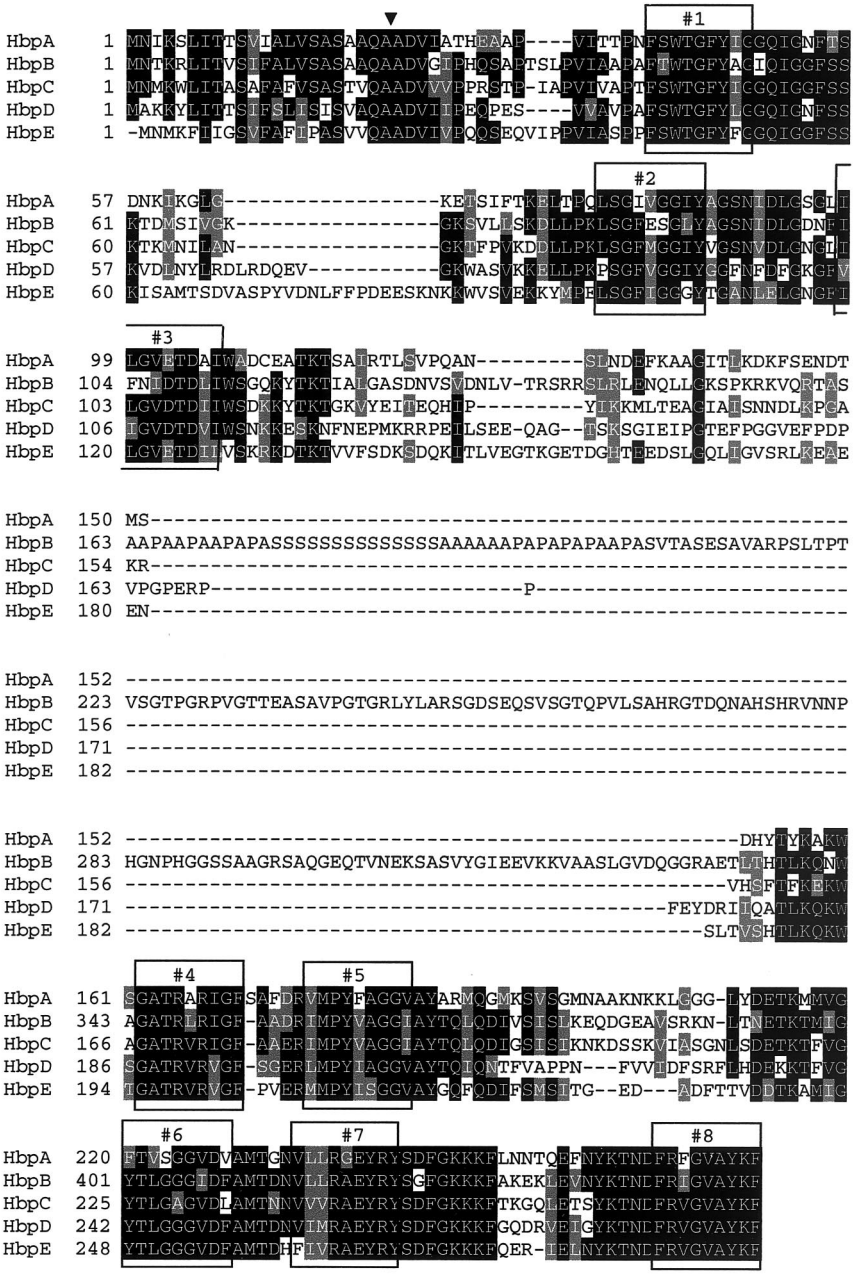

FIG. 2. Multiple sequence alignment of the five Hbp family members. Identical residues are shaded in black; conserved residues are shaded in gray. Predicted β-strand transmembrane domains are boxed and numbered. Transmembrane domains 5, 6, 7, and 8 are nearly identical to those in neisserial Opa proteins (15). The secretory signal sequence cleavage sites (as determined for HbpA [6] and HbpD [this study]) are indicated by an arrowhead.

peats (Fig. 1B). Without this insert, *hbpB* would be similar in length to other *hbp* family members. It is also interesting that the insert has an elevated G+C content relative to other genes in the *B. quintana* genome (~50% versus 39% G+C [28]), including the other *hbp* genes. In addition, *hbpB* sequences that flank the insert have a typical G+C content for a *B. quintana* gene.

A multiple sequence alignment of the predicted proteins encoded by the *hbp* gene family reveals a high degree of amino acid sequence conservation (Fig. 2). The average sequence identity between Hbp family members is 48% (excluding HbpB). Each protein contains a predicted secretory signal sequence (see Fig. 2) as described for HbpA (6) and HbpD (this study) and contains a terminal phenylalanine. The prominent 36-kDa protein previously shown to copurify with HbpA in Triton X-114 extracts of *B. quintana* (6) was identified as HbpD by N-terminal sequencing. The N-terminal sequence of mature HbpD was determined to be ADVIIPEQPESV-VAVPAFS, a perfect match to the predicted HbpD sequence shown in Fig. 2.

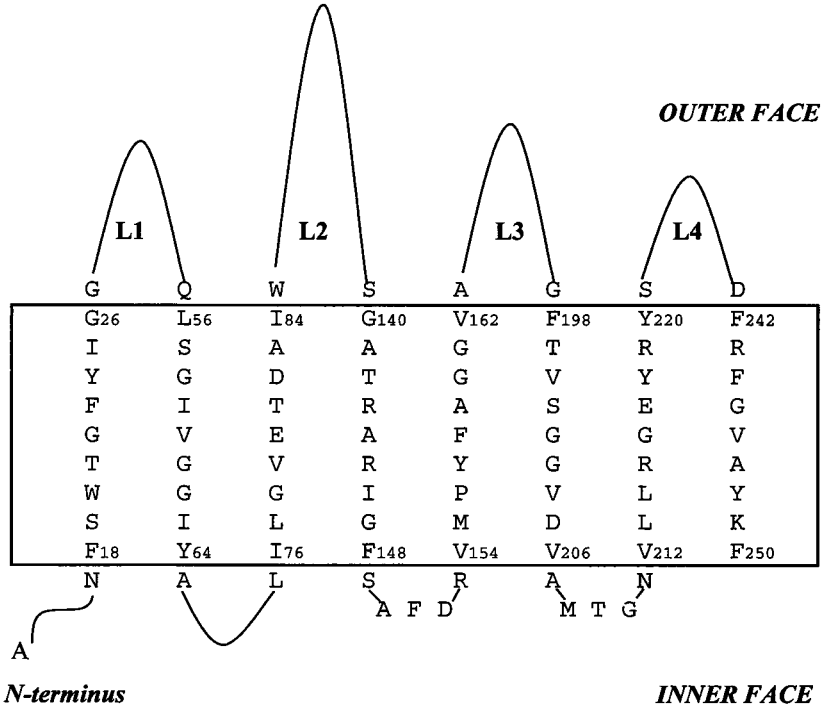

FIG. 3. Predicted two-dimensional β-barrel structure for HbpA. The inner and outer faces of the outer membrane are indicated. The bold residues (shifted to the right) indicate the nonpolar side of the eight transmembrane β strands. The transmembrane domains correspond to those boxed in Fig. 3.

Homologs from other bacteria. BLAST searches revealed that the closest homologs in the database (greatest to least) include *B. henselae* PAP31 (phage-associated/membrane protein [4]), *Brucella* OMP31 (putative porin [29, 30]), and *A. tumefaciens* OMP25 (immunogenic surface protein [9]). Sequence identities to HbpA range from 32% (OMP31) to 58% (Pap31). The function(s) of these related surface proteins has not been fully elucidated, and their widespread occurrence in several plant and animal pathogens within the α-proteobacteria warrants further investigation. BLASTp searches with Hbps also generated numerous "hits" on the neisserial opacity (Opa) proteins. Although the overall sequence identity value between Hbps and Opa is only about 25%, the Hbp family members are approximately 40% similar to Opa, and considerable identity to Opa is observed in the last quarter of the Hbp molecule indicated by a Opa conserved domain (not shown).

Secondary structure model for HbpA. Given the similarity between Opa and Hbps and the fact that the last four predicted transmembrane domains of HbpA to -E (see boxes 5, 6, 7, and 8 in Fig. 2) are nearly identical to those predicted in the two-dimensional model for Opa (15), a two-dimensional model of HbpA was generated using the methodology applied to Opa (15). The resulting β-barrel model for HbpA contains eight transmembrane domains, the last terminating with a phenylalanine (Fig. 3). As is typical of outer membrane protein families, the predicted transmembrane strands for the Hbps correspond to the most-conserved sequences among the family members (Fig. 2) and likely serve as framework regions (10). The two-dimensional model for HbpA also indicates that the largest loops of the protein are extracellular, whereas the short loops are intracellular. An excellent example of this is the unusually large L2 loop that is predicted for HbpB, corresponding to the 510-bp GC-rich insert containing the variable number tandem repeat (Fig. 1). The predicted transmembrane domains of HbpA are antiparallel amphipathic β strands as found in porins (8, 31) and in Opa (15). Many of the predicted β strands of Hbp (Fig. 2 and 3) are flanked by aromatic residues; a characteristic of β strands that span outer membranes (8, 31). Similar models can also be generated from the other Hbp family members (not shown), implying a conserved structure.

Expression of *hbp* family members. In vitro transcription-translation of cloned *hbp* genes shows that the apparent molecular masses for the Hbp proteins as determined by SDS-PAGE and/or autoradiographic analysis (not shown) are in close agreement with values from predicted amino acid sequences, with values of ~ 30 and 29.3 kDa (HbpA), 55.9 and 47.1 kDa (HbpB), 28.6 and 30.1 kDa (HbpC), 26.5 and 32.7 kDa (HbpD), and 35.1 and 33 kDa (HbpE), respectively. We attribute the discrepancy in HbpB values to aberrant SDS-PAGE migration resulting from its large and unusual insert sequence. Another discrepancy was observed between mature HbpD produced in vivo in *B. quintana* (~36 kDa) (6) and recombinant, immature HbpD produced in vitro (26.5 kDa). The expected value for immature HbpD should be ca. 2.4 kDa greater than the mature protein by virtue of its intact signal sequence.

RT-PCR was performed to quantify relative expression levels of the *hbp* family members during bacterial growth on standard medium (HIAB). The data clearly show that all *hbp*

TABLE 3. Real-time PCR[a] of hemin-binding protein gene family in wild-type and *hbpA* mutant in *B. quintana*

Target gene	Wild type		Mutant		ΔC_{Tq}[c] (avg)	$\Delta\Delta C_T$[d]	Fold difference in mutant relative to wild type ($2^{-\Delta\Delta C_T}$)
	RNA amt[b] (ng)	Avg $C_T \pm$ SEM	RNA amt[b] (ng)	Avg $C_T \pm$ SEM			
16s rRNA	1.25	10.67 ± 0.11	1.25	11.79 ± 0.25	1.12 (1.40)	0.00	1.00
	0.625	12.00 ± 0.08	0.625	13.35 ± 0.06	1.35		
	0.313	12.86 ± 0.13	0.313	14.60 ± 0.24	1.74		
hbpC	1.25	25.57 ± 0.15	1.25	25.21 ± 0.11	−0.36 (−0.40)	−1.80	3.48 (increased in mutant)
	0.625	26.66 ± 0.11	0.625	26.28 ± 0.15	−0.38		
	0.313	27.64 ± 0.18	0.313	27.19 ± 0.13	−0.45		
hbpA	1.25	22.08 ± 0.05	1.25	25.27 ± 0.06	3.19 (3.13)	1.73	−3.33 (decreased in mutant)
	0.625	23.29 ± 0.04	0.625	26.39 ± 0.07	3.10		
	0.313	24.29 ± 0.02	0.313	27.40 ± 0.04	3.11		
hbpB	1.25	30.02 ± 0.10	1.25	29.77 ± 0.16	−0.25 (−0.44)	−1.84	3.58 (increased in mutant)
	0.625	31.25 ± 0.13	0.625	30.68 ± 0.19	−0.57		
	0.313	32.58 ± 0.10	0.313	32.08 ± 0.14	−0.50		
hbpD	1.25	21.13 ± 0.05	1.25	18.85 ± 0.02	−2.28 (−2.38)	−3.78	13.74 (increased in mutant)
	0.625	22.02 ± 0.10	0.625	19.78 ± 0.04	−2.24		
	0.313	23.44 ± 0.10	0.313	20.81 ± 0.14	−2.63		
hbpE	1.25	26.14 ± 0.06	1.25	25.04 ± 0.01	−1.10 (−1.17)	−2.57	5.94 (increased in mutant)
	0.625	27.27 ± 0.02	0.625	25.97 ± 0.05	−1.30		
	0.313	28.30 ± 0.10	0.313	27.20 ± 0.06	−1.10		

[a] Reactions were performed in triplicate.
[b] That is, the nanogram amount of total RNA per 10-μl reaction.
[c] That is, the average mutant C_T - the average wild-type C_T. The average of all three values for each gene is given in parentheses.
[d] That is, the average ΔC_{Tq} minus the average ΔC_{Tq} for 16S rRNA.

family members are expressed under routine culture conditions. Further, a comparison of relative expression levels based on C_T values reveals that *hbp* transcripts are produced in the following order (most abundant to rarest): *hbpD*, *hbpA*, *hbpC*, *hbpE*, and *hbpB* (Table 3).

Effect of *hbpA* mutagenesis on the hemin-binding phenotype. *B. quintana hbpA* mutants were generated via allelic exchange after electroporation of pHBPA′ suicide vector into strain LS200. One resulting mutant, strain LS300, was isolated from HIAB-Kan plates, and its mutation was verified by PCR analysis of *hbpA* (not shown) as previously described (3, 7). The protein profile for LS300 was also examined by SDS-PAGE, and immunoblots were developed with rabbit anti-HbpA, as previously described (6). The data clearly show that the prominent 30-kDa HbpA band in LS200 is absent in the protein profile of LS300 (Fig. 4A, lanes 2 and 3, respectively). Further, HbpA or a truncated version of the protein cannot be detected in the LS300 lysate by immunoblot analysis (Fig. 4B, lane 3). Complementation of LS300 in *trans* reestablished synthesis of the HbpA protein to levels ca. 5% of the parental strain, LS200, and detection was limited to immunoblots (Fig. 4B, lane 4). This is the first report of site-directed mutation and *trans*-complementation in *B. quintana*.

To gauge the effect of the *hbpA* mutation on the hemin-binding phenotype of *B. quintana*, an in vitro hemin-binding assay was done as previously described (6). Much to our surprise, data from this assay showed that the LS300 *hbpA* mutant actually exhibits a significantly higher level of hemin-binding relative to the LS200 parental strain (16 ± 0.5 versus 10.3 ± 0.25 μg/mg of protein, respectively), whereas the LS400 *trans*-complemented strain exhibits an intermediate phenotype (12.4 ± 0.5 μg/mg of protein) (Fig. 5).

Quantitative RT-PCR analysis of wild-type versus mutant. The relative transcript levels of the *hbp* gene family in the wild-type and *hbpA* mutant in *B. quintana* were assessed by quantitative RT-PCR. The results are summarized in Table 3.

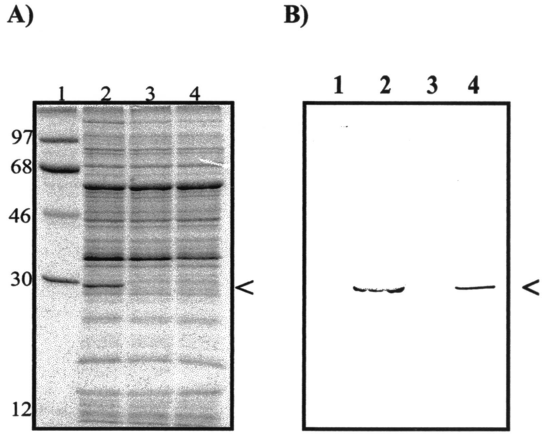

FIG. 4. Analysis of HbpA synthesis in a *B. quintana hbpA* mutant and *trans*-complemented strain. (A) Coomassie blue-stained SDS-PAGE gel containing cell lysates of the LS200 parental strain (lane 2), the *hbpA* mutant LS300 (lane 3) and the *trans*-complemented strain LS400 (lane 4). (B) Corresponding immunoblot. The HbpA protein is indicated by an arrowhead. Molecular mass standards (lane 1) are indicated to the left in kilodaltons.

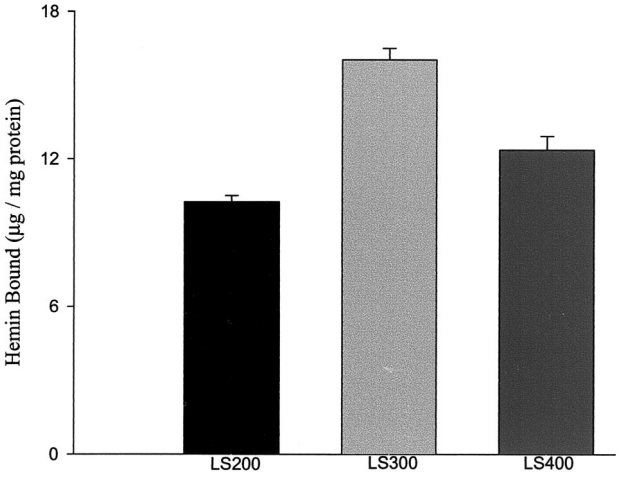

FIG. 5. Hemin-binding assay of parental (LS200), *hbpA* mutant (LS300), and *trans*-complemented (LS400) strains of *B. quintana*. Data are expressed as the means plus the standard error of the mean for eight assays.

When C_T values were normalized to 16S rRNA, we determined that the transcription levels of *hbpB* and *hbpC* were increased 3.58- and 3.48-fold, respectively, in the mutant relative to the wild type. Even more striking was the observation that *hbpE* and *hbpD* were increased 5.94- and 13.74-fold, respectively, in the mutant compared to the wild type. If these homologs share receptor function, the significant increase in the level of transcription by the other four gene family members may explain the enhancement in hemin binding seen in the *hbpA* mutant.

RT-PCR also showed that *hbpA* expression was apparently decreased by 3.33-fold in the mutant (Table 3). We ascribe this moderate level of expression to two observations. First, Northern blot analysis using RNA from wild-type and mutant strains reveals a readthrough transcript of approximately 850 bp in the mutant versus a 1,000-bp message in the wild type (data not shown). It is likely that a promoter on the suicide vector-based insert is responsible. Second, the RT-PCR target region (nucleotides 647 to 718) is located 3′ to the mutational target (nucleotides 344 to 583), making this transcript detectable.

DISCUSSION

B. quintana has the highest reported hemin requirement for bacterial growth in vitro (20 to 40 μg per ml of medium [17]). However, the reason for this extraordinary hemin requirement and the mechanisms involved in its acquisition are poorly characterized. In a previous study, we identified eight membrane-associated proteins in *B. quintana* that bind hemin in vitro (6). Of these, the most prominent was a 30-kDa outer membrane protein, HbpA, that appears to play a role as a hemin receptor for the pathogen.

Chromosomal walking of sequences that flank *hbpA* led to the discovery of two paralagous genes, which we termed *hbpB* and *hbpC* (Fig. 1). Sequence data obtained from the *B. quintana* genome project (University of Uppsala, Uppsala, Sweden) identified two additional, unlinked homologues termed *hbpD* and *hbpE*. Each of the five *hbp* genes, including the closely linked *hbpCAB* genes, possesses endogenous promoter regions, as demonstrated by expression in vitro from plasmids containing directionally cloned inserts in opposition to the *lacZ* promoter of the multiple cloning site. Further, these genes contain potential *fur* regulatory elements as previously described for *hbpA* (6), suggesting that they may be regulated by Fur. This is the first report of a multigenic family in *Bartonella*.

Members of the *hbp* gene family encode homologs that share approximately 50% amino acid sequence identity (Fig. 2), suggesting that structure and function may also be conserved. We hypothesize that all Hbp family members are located in the outer membrane based upon: (i) their considerable homology to HbpA, a known outer membrane protein (6); (ii) possession of a C-terminal phenylalanine (25); and (iii) a predicted (HbpB, -C, and -E) or verified (HbpA and -D) secretory signal sequence (Fig. 2).

Although the majority of Hbp family members are approximately 30 kDa, the HbpB protein is nearly 56 kDa due to an ~510-bp insert in its respective gene. The insert is interesting by virtue of its 14 nested variable-number tandem repeats (Fig. 1B) and its aberrantly high GC richness compared to the *B. quintana* genome (~50 versus 39% G+C; [28]). These features suggest that the element was derived from a foreign source such as a phage or transposable element. A second incongruity was observed between the molecular mass of recombinant, immature HbpD produced in vitro with that observed for mature HbpD isolated from Triton X-114 extracts of *B. quintana* (36 kDa [6]). It is possible that this disparity results from posttranslational modification of HbpD in *Bartonella*.

Numerous homologs of the Hbp proteins were identified by using BLAST searches, and many of these are surface proteins from closely related pathogenic α-proteobacteria (e.g., *Brucella* and *Agrobacterium*). It is tempting to speculate that these homologs, together with the Hbp family, comprise a superfamily of related outer membrane proteins that may share at least some functions. One interesting homolog identified by BLAST searches was the neisserial Opa. A secondary structure prediction for HbpA reveals a potential β-barrel structure containing eight transmembrane domains, four extracellular loops, and three intracellular loops. The predicted transmembrane domains are highly conserved in all Hbp family members (Fig. 2), and similar predictions can be made with other Hbp proteins (data not shown). Studies to verify this predicted topology are currently under way in our laboratory.

The existence of a multigene Hbp family in *Bartonella* might provide the pathogen with redundant "backup" systems for facilitating hemin acquisition or some other unknown function(s). Undoubtedly, many of the conserved regions of these molecules may be more closely related to structure than function. For example, the predicted conserved transmembrane domains may simply serve to anchor the extracellular loop domains for their designed activity.

Mutagenesis of *hbpA* was done in order to examine the effect of mutation on the hemin-binding phenotype of *B. quintana* and to establish a system of genetic manipulation for this bacterium. Using allelic exchange, we successfully mutagenized *hbpA* with a suicide vector. In addition, *trans*-complementation of the mutation with a shuttle vector was accomplished. The resulting strains were subsequently analyzed for their hemin-

binding phenotype in vitro. We discovered that mutagenesis of *hbpA* actually rendered a strain that bound 56% more hemin than the parental strain, whereas reestablishment of *hbpA* expression in *trans* (to levels ca. 5% that of the parental strain) provided an intermediate phenotype (Fig. 5).

Although the hemin-binding assay measures both receptor and non-receptor-mediated binding, enhanced hemin binding by the *hbpA* mutant led us to hypothesize that alterations in the expression of the other *hbp* family members might be responsible for this phenotype. To investigate this possibility, we performed quantitative RT-PCR with RNA extracted from the wild type and the *hbpA* mutant. The results summarized in Table 3 suggest that *hbpB*, *hbpC*, *hbpD*, and *hbpE* are all upregulated in the mutant relative to the wild-type strain, even as high as 13.74-fold in the case of *hbpD*. Although it is possible that altered surface characteristics (e.g., hydrophobicity or charge) or other non-receptor-mediated hemin binding may be responsible for this observation (Fig. 5), the clear and significant upregulation of *hbp* family members suggests that a compensatory expression is taking place. This observation, coupled with the family's conservation in predicted structure and possession of putative Fur regulatory elements, suggests that other *hbp* gene products may also serve as hemin receptors. This hypothesis is currently under investigation in our laboratory.

This is the first multigene family described from a *Bartonella* species. As such, it presents a unique opportunity to investigate differential gene regulation in this poorly characterized bacterium. In addition, the hypothesized role for additional *hbp* family members in hemin binding underscores the potential importance of this gene family for virulence.

ACKNOWLEDGMENTS

We thank Patty McIntire at The University of Montana Murdock Molecular Biology Facility for sequence analyses, Mark Garfield at the Twinbrook II Facility at NIH for peptide sequencing, and Russ Regnery for *B. quintana*.

M.F.M. was supported by Public Health Service grant AI45534 and American Heart Established Investigator grant 9940002N. J.A.C. was supported through a NIH-NIAID Intramural Research Training Award. K.R.S was supported through an NSF-EPSCoR undergraduate fellowship.

REFERENCES

1. **Altschul, S. F., W. Gish, W. Miller, E. W. Myers, and D. J. Lipman.** 1990. Basic local alignment search tool. J. Mol. Biol. **215:**403–410.
2. **Ausubel, F. M., R. Brent, R. E. Kingston, D. D. Moore, J. G. Seidman, J. A. Smith, and K. Struhl.** 1995. Current protocols in molecular biology. John Wiley & Sons, Inc., New York, N.Y.
3. **Battisti, J. M., and M. F. Minnick.** 1999. Development of a system for genetic manipulation of *Bartonella bacilliformis*. Appl. Environ. Microbiol. **65:**3441–3448.
4. **Bowers, T. J., D. Sweger, D. Jue, and B. Anderson.** 1998. Isolation, sequencing and expression of the gene encoding a major protein from the bacteriophage associated with *Bartonella henselae*. Gene **206:**49–52.
5. **Byam, W.** 1919. Trench fever, p. 120–130. *In* L. L. Lloyd (ed.), Lice and their menace to man. Oxford University Press, Oxford, United Kingdom.
6. **Carroll, J. A., S. A. Coleman, L. S. Smitherman, and M. F. Minnick.** 2000. Hemin-binding surface protein from *Bartonella quintana*. Infect. Immun. **68:**6750–6757.
7. **Coleman, S. A., and M. F. Minnick.** 2001. Establishing a direct role for the *Bartonella bacilliformis* invasion-associated locus B (IalB) protein in human erythrocyte parasitism. Infect. Immun. **69:**4373–4381.
8. **Cowan, S. W., T. Schirmer, G. Rummel, M. Steiert, R. Ghosh, R. A. Pauptit, J. N. Jansonius, and J. P. Rosenbusch.** 1992. Crystal structures explain functional properties of two *E. coli* porins. Nature **358:**727–733.
9. **Goodner, B., G. Hinkle, S. Gattung, N. Miller, M. Blanchard, B. Qurollo, et al.** 2001. Genome sequence of the plant pathogen and biotechnology agent *Agrobacterium tumefaciens*. Science **294:**2323–2328.
10. **Jeanteur, D., J. Lakey, and F. Pattus.** 1994. The porin superfamily: diversity and common features, p. 363–380. *In* J. M. Ghuysen and R. Hakenbeck (ed.), Bacterial cell wall. Elsevier, Amsterdam, The Netherlands.
11. **Jackson, L. A., and D. H. Spach.** 1996. Emergence of *Bartonella quintana* infection among homeless persons. Emerg. Infect. Dis. **2:**141–144.
12. **Jackson, L. A., D. H. Spach, D. A. Kippen, N. K. Sugg, R. L. Regnery, M. H. Sayers, and W. E. Stamm.** 1996. Seroprevalence to *Bartonella quintana* among patients at a community clinic in downtown Seattle. J. Infect. Dis. **173:**1023–1026.
13. **Koehler, J. E., F. D. Quinn, T. G. Berger, P. E. LeBoit, and J. W. Tappero.** 1992. Isolation of *Rochalimaea* species from cutaneous and osseous lesions of bacillary angiomatosis. N. Engl. J. Med. **327:**1625–1631.
14. **Livak, K. J., and T. D. Schmittgen.** 2001. Analysis of relative gene expression data using real-time quantitative PCR and the $2^{-\Delta\Delta C_T}$ method. Methods **25:**402–408.
15. **Malorny, B., G. Morelli, B. Kusecek, J. Kolberg and M. Achtman.** 1998. Sequence diversity, predicted two-dimensional protein structure and epitope mapping of neisserial Opa proteins. J. Bacteriol. **180:**1323–1330.
16. **Matsudaira, P.** 1987. Sequence from picomole quantities of proteins electroblotted onto polyvinylidene difluoride membranes. J. Biol. Chem. **262:** 10035–10038.
17. **Myers, W. F., L. D. Cutler, and C. L. Wisseman.** 1969. Role of erythrocytes and serum in the nutrition of *Rickettsia quintana*. J. Bacteriol. **97:**663–666.
18. **Parrott, J. H., L. Dure, W. Sullender, W. Buraphacheep, T. A. Frye, C. A. Galliani, E. Marston, D. Jones, and R. Regnery.** 1997. Central nervous system infection associated with *Bartonella quintana*: a report of two cases. Pediatrics **100:**403–408.
19. **Pearson, W. R.** 1990. Rapid and sensitive sequence comparison with FASTP and FASTA. Methods Enzymol. **183:**63–98.
20. **Reschke, D. K., M. E. Frazier, and L. P. Mallavia.** 1990. Transformation of *Rochalimaea quintana*, a member of the family *Rickettsiaceae*. J. Bacteriol. **172:**5130–5134.
21. **Sambrook, J., E. F. Fritsch, and T. Maniatis.** 1989. Molecular cloning: a laboratory manual, 2nd ed. Cold Spring Harbor Laboratory, Cold Spring Harbor, N.Y.
22. **Scherer, D. C., I. DeBuron-Connors, and M. F. Minnick.** 1993. Characterization of *Bartonella bacilliformis* flagella and effect of antiflagellin antibodies on invasion of erythrocytes. Infect. Immun. **61:**4962–4971.
23. **Spach, D. H., K. P. Callis, D. S. Paauw, Y. B. Houze, F. D. Schoenknecht, D. F. Welch, H. Rosen, and D. J. Brenner.** 1993. Endocarditis caused by *Rochalimaea quintana* in a patient infected with human immunodeficiency virus. J. Clin. Microbiol. **31:**692–694.
24. **Spach, D. H., A. S. Kanter, M. J. Dougherty, A. M. Larson, M. B. Coyle, D. J. Brenner, B. Swaminathan, G. M. Matar, D. F. Welch, R. K. Root, and W. E. Stamm.** 1995. *Bartonella* (*Rochalimaea*) quintana bacteremia in inner-city patients with chronic alcoholism. N. Engl. J. Med. **332:**424–428.
25. **Struyve, M., M. Moons, and J. Tommassen.** 1991. Carboxy-terminal phenylalanine is essential for the correct assembly of a bacterial outer membrane protein. J. Mol. Biol. **218:**141–148.
26. **Thompson, J. D., D. G. Higgins, and T. J. Gibson.** 1994. CLUSTAL W: improving the sensitivity of progressive multiple sequence alignment through sequence weighting, position-specific gap penalties and weight matrix choice. Nucleic Acids Res. **22:**4673–4680.
27. **Towbin, H., T. Staehelin, and J. Gordon.** 1979. Electrophoretic transfer of proteins from polyacrylamide gels to nitrocellulose sheets: procedure and some applications. Proc. Natl. Acad. Sci. USA **76:**4350–4354.
28. **Tyeryar, F. J., E. Weiss, D. B. Millar, F. M. Bozeman, and R. A. Ormsbee.** 1973. DNA base composition of rickettsiae. Science **180:**415–417.
29. **Vizcaino, N., A. Cloeckaert, M. S. Zygmunt, and G. Dubray.** 1996. Cloning, nucleotide sequence, and expression of the *Brucella melitensis omp31* gene coding for an immunogenic major outer membrane protein. Infect. Immun. **64:**3744–3751.
30. **Vizcaino, N., J. M. Verger, M. Grayon, M. S. Zygmunt, and A. Cloeckaert.** 1997. DNA polymorphism at the *omp-31* locus of *Brucella* spp.: evidence for a large deletion in *Brucella aborutus*, and other species-specific markers. Microbiology **143:**2913–2921.
31. **Weiss, M. S., U. Abele, J. Weckesser, W. Welte, E. Schiltz, and G. E. Schulz.** 1991. Molecular architecture and electrostatic properties of a bacterial porin. Science **254:**1627–1630.
32. **Weiss, E., and G. A. Dasch.** 1982. Differential characteristics of strains of *Rochalimaea*: *Rochalimaea vinsonii* sp. nov., the Canadian vole agent. Int. J. Syst. Bacteriol. **32:**305–314.

Editor: D. L. Burns